

Exascale Simulations of Fusion and Fission Systems

Misun Min^{a,*}, Yu-Hsiang Lan^{a,e}, Paul Fischer^{a,e,f}, Elia Merzari^{b,g}, Tri Nguyen^b, Haomin Yuan^g, Patrick Shriwise^c, Stefan Kerkemeier^a, Andrew Davis^d, Aleksandr Dubas^d, Rupert Eardly^d, Rob Akers^d, Thilina Rathnayake^e, Tim Warburton^h

^aMathematics and Computer Science, Argonne National Laboratory, Lemont, IL 60439

^bDepartment of Nuclear Engineering, Penn State, University Park, PA 16802

^cComputational Science, Argonne National Laboratory, Lemont, IL 60439

^dUnited Kingdom Atomic Energy Authority, Culham Science Centre, Abingdon, Oxfordshire, OX14 3DB, United Kingdom

^eDepartment of Computer Science, University of Illinois at Urbana-Champaign, Urbana, IL 61801

^fDepartment of Mechanical Science and Engineering, University of Illinois at Urbana-Champaign, Urbana, IL 61801

^gNuclear Science and Engineering, Argonne National Laboratory, Lemont, IL 60439

^hDepartment of Mathematics, Virginia Tech, Blacksburg, VA 24061

Abstract

We discuss pioneering heat and fluid flow simulations of fusion and fission energy systems with NekRS on exascale computing facilities, including Frontier and Aurora. The Argonne-based code, NekRS, is a highly-performant open-source code for the simulation of incompressible and low-Mach fluid flow, heat transfer, and combustion with a particular focus on turbulent flows in complex domains. It is based on rapidly convergent high-order spectral element discretizations that feature minimal numerical dissipation and dispersion. State-of-the-art multilevel preconditioners, efficient high-order time-splitting methods, and runtime-adaptive communication strategies are built on a fast OCCA-based kernel library, libParanumal, to provide scalability and portability across the spectrum of current and future high-performance computing platforms. On Frontier, Nek5000/RS has achieved an unprecedented milestone in breaching over 1 trillion degrees of freedom with the spectral element methods for the simulation of the CHIMERA fusion technology testing platform. We also demonstrate for the first time the use of high-order overset grids at scale.

Keywords: Fusion, Fission, CHIMERA, Nek5000, NekRS, Spectral Element, Overset Grids, Exascale

1. Introduction

Advanced fission and fusion energy hold promise as a reliable, carbon-free energy source capable of meeting the United States' commitments to addressing climate change. A wave of investment in fission and fusion power within the United States and worldwide indicates an important maturation of academic research projects into the commercial space. Nonetheless, the design, certification, and licensing of novel fission and fusion concepts pose formidable hurdles to successfully deploying new technologies. Because of the high cost of integral-effect nuclear experiments, high-fidelity numerical simulation is poised to play a crucial role in these efforts.

Within the DOE's Exascale Computing Project (ECP), the ExaSMR program developed high-confidence numerical methods such as computational fluid dynamics (CFD) for thermal-fluid heat

and momentum transport. The project successfully executed these simulations on exascale systems and generated highly detailed virtual datasets of operational and advanced concept nuclear reactors, which have the potential to impact a wide range of reactor designs. The results of our simulation campaigns and the achieved performance improvements were summarized in a recent article [1]. *In the present article, we further extend those fission reactor results, including, for the first time, results on Aurora. We also introduce the first exascale simulation of a facility representative of a fusion breeding blanket, which presents engineering challenges similar to fission systems.*

Historically, because of the complexity and range of scales involved in turbulent flow (1 μm –10 m), simplifications involving Reynolds averaging have been necessary. Such approaches, while powerful and useful for design, require modeling closures that are expensive or impossible to develop and validate, especially at the appropriate scale, and lead to design compromises in terms of operational margins and economics.

*Corresponding author

Email address: mmin@mcs.anl.gov (Misun Min)

Under ECP, the NekRS code, a GPU-enabled spectral element solver for heat and fluid flow, was developed and deployed to all major GPU architectures [2], leading to transformative changes in the realm of what can be simulated with the introduction of restrictive assumptions. To understand the transformative leap enabled by NekRS, it is instructive to examine simulations in pebble beds. Before NekRS, the largest pebble bed calculations in the literature were of the order of 1000 pebbles. In 2022 we reported calculations involving the full Mark-I Fluoride Cooled High Temperature Reactor core (352,625 pebbles) [3]. Recently, these achievements were extended to simulations involving radiation transport for a full small modular reactor core involving actually a considerably larger mesh size [1] breaching for the first time the billion spectral element barrier. We also note that, throughout the ECP, NekRS has been tested and deployed on three generations of GPU-based supercomputers.

Fusion breeding blankets are crucial components in nuclear fusion devices, designed to harness the energy produced during fusion reactions. These blankets surround the core where fusion occurs, serving multiple essential functions: they help manage heat transfer, providing thermal insulation and converting heat into usable energy; they protect the reactor structure from intense neutron radiation; and they breed tritium. Breeding blankets use materials like lithium to absorb neutrons from the fusion process, which transmute into more tritium, completing the fusion energy fuel cycle. This technology is key to making fusion power a viable and sustainable energy source, but it presents several challenges. Materials are subject to an intense radiation field and subject to radiation damage. Moreover, the heat flux encountered at the first wall and in the divertor are very intense and among the highest possible, creating a challenging environment [4, 5].

To test various technology candidates, the CHIMERA [6] fusion technology facility will enable the testing of large in-vessel component modules under fusion reactor-like conditions of combined in-vacuum thermal power density and magnetic field. With an integral large superconducting magnet and a pressurized water loop, CHIMERA is also ideally placed for experiments on liquid metal breeding blanket prototypes. An infrared heating system has been developed, capable of applying $0.5 MW/m^2$ to component surfaces up to the size of the ITER test blanket module first wall. The modules of this heater are highly specialised and designed to endure the high magnetic forces from the CHIMERA static and pulsed magnets. CHIMERA will feature a range of diagnostics, including load cells to measure static and pulsed magnetic forces, and induced current sensors, all of which have been tested to confirm

acceptable operation in the pulsed magnetic field. A high-fidelity numerical tool of CHIMERA will support the scientific and engineering goals being pursued. *We present first-of-a-kind turbulent flow and heat transfer simulations of CHIMERA. Results are shown in Fig. 1.*

CHIMERA includes a complex high Reynolds-number piping system involving several manifolds and connections. It also involves multiple heating plates and an infrared system to simulate the intense heat flux of first-wall conditions. The geometry is exceedingly complex. Generating an adequate discretization posed significant challenges. *To model the system, an overset grid multi-domain approach was used in which solid and fluid domains are meshed separately, and information is transferred between the two by interpolation at the boundary [7, 8]. This manuscript represents the first exascale demonstration of this technique.*

To investigate the performance of NekRS on Frontier and Aurora, we discuss two numerical models:

- A portion of a fission core for a Small Modular Reactor.
- The CHIMERA model (Fig. 1).

Fission core. The core consists of 37 assemblies, each having a 17×17 lattice of fuel pins and guide tubes, with the guide tubes placed in standard positions. This full-core configuration was modeled in previous publications [9, 1] and featured 37 identical assemblies with the same 17×17 configuration. Runs were conducted with up to $6.03 \cdot 10^{11}$ grid points. *In this work, we consider only a subset of the problem, a single assembly (17×17 configuration), to continue benchmarking the code against novel architectures.* The current fluid mesh for each assembly has $E = 27,700$ fluid elements per two-dimensional layer and $E = 31,680$ solid elements per 2D layer. Multiple extrusions are considered. The fluid properties used in the simulations were evaluated at 553 K, and an incompressible formulation was chosen due to the small changes in density for the problem of interest. The energy equation is solved in its temperature form. While the geometry is extruded, each pin has a unique spatially dependent power profile and composition, making the problem three-dimensional. The work was largely presented in [1] for Frontier, but here we present novel results on Aurora.

CHIMERA model. The mesh for the CHIMERA facility has up to $E = 1,691,729,664$ elements for the piping system and $E = 55,056,380$ in the solid. Several smaller meshes for the piping system were also designed to study scalability. The largest mesh is designed for wall-resolved Large Eddy Simulation and Direct Numerical Simulation of the flow

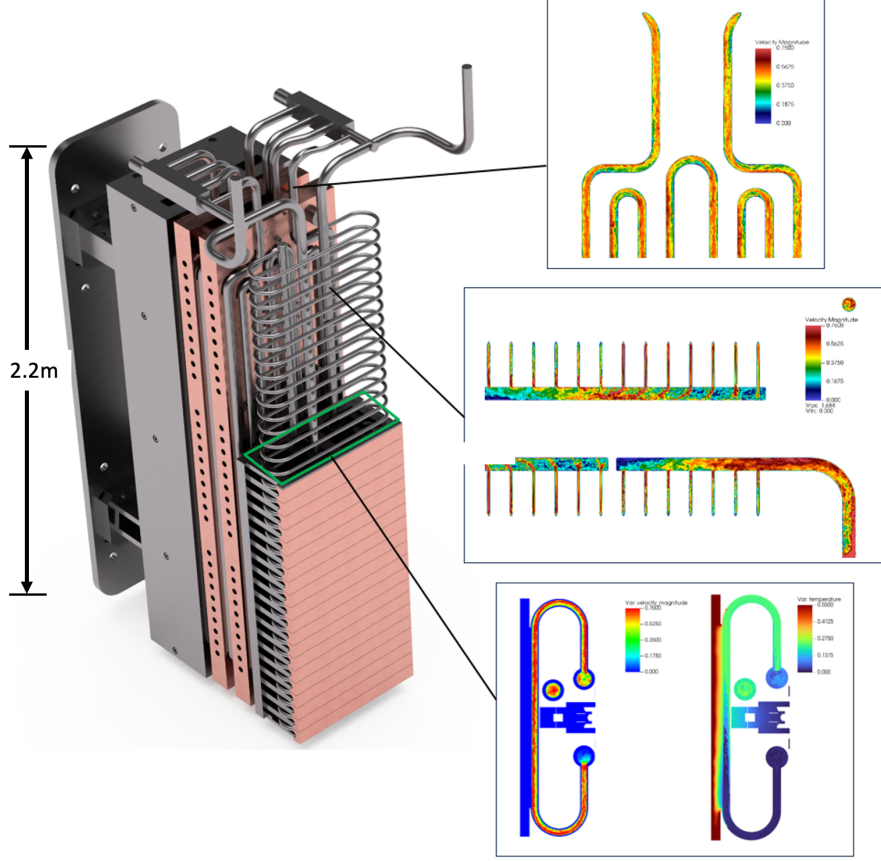


Figure 1: Rendering of the CHIMERA facility with NekRS simulation results for velocity and temperature.

at $Re = 10^5 - 10^6$, resolving the boundary layer everywhere in the piping. **This translates into over $1.1 \cdot 10^{12}$ grid points at polynomial order $N = 9$, the largest simulation ever attempted with the spectral element methods and one of the largest fluid simulations in a complex geometry to date.** Inlet-outlet boundary conditions are applied. In the solid, a heat flux is applied on the outer surface (i.e., first wall simulator). Heat loads are also applied on some of the heat transfer plates, which are illustrated in the 3D relief of Fig. 1.

We emphasize that the work presented here is a considerable leap in problem size, geometry complexity and simulation complexity (overset grids) compared to our previous submission [1].

2. Formulations

Heat and Mass transfer are the key mechanisms for power generation in fusion and fission systems. The problem is governed by the incompressible Navier-Stokes equations (NSE) for velocity (\mathbf{u}) and pressure (p) coupled with the temperature (T) equation,

$$\frac{DT}{Dt} := \frac{\partial T}{\partial t} + \mathbf{u} \cdot \nabla T = \frac{1}{Re \cdot Pr} \nabla^2 T + q \quad (1)$$

$$\frac{D\mathbf{u}}{Dt} := \frac{\partial \mathbf{u}}{\partial t} + \mathbf{u} \cdot \nabla \mathbf{u} = \frac{1}{Re} \nabla^2 \mathbf{u} - \nabla p, \quad \nabla \cdot \mathbf{u} = 0, \quad (2)$$

where $Re = UL/\nu \gg 1$ is the Reynolds number based on flow speed U , length scale L , and viscosity ν , and Pr is the Prandtl number (i.e., the ratio of momentum to thermal diffusivities) and q is the volumetric heat deposition coming from radiation transport calculations. From a computational standpoint, the long-range coupling of the incompressibility constraint, $\nabla \cdot \mathbf{u} = 0$, makes the pressure sub-step intrinsically communication intensive and a major focus of our effort as it can easily consume 60-80% of the run time [3]. We note that in solids, only the temperature equation is solved and without the advection term.

NekRS is based on the spectral element method (SEM) [10], in which functions are represented as N th-order polynomials on each of E elements, for a total mesh resolution of $n = EN^3$. It originates from two code suites: Nek5000 [11], which is a 1999 Gordon Bell winner [12], and libParanumal [13, 14], which is a fast GPU-oriented library for high-order methods written in the Open Concurrent Computing Abstraction (OCCA) for cross-platform portability [15]. OCCA provides backends for CUDA, HIP, DPC++, and OpenCL with virtually no performance degradation over native implementations.

Direct numerical simulation (DNS) and large-

eddy simulation (LES) of turbulence typically require simulations over long times to gather statistics. Campaigns that can last weeks require not only performant implementations but also *efficient discretizations* that deliver high accuracy at low cost per gridpoint. Kreiss and Olinger noted early on the importance of high-order methods when considering long integration times [16]. To offset cumulative dispersion errors, $e(t) \sim Ct$, one must have $C \ll 1$ when $t \gg 1$. **For this reason, SEM offers several advantages for the high-fidelity modeling of turbulent heat and fluid flow.**

SEM accommodates body-fitted coordinates through isoparametric mappings of the reference element, $\hat{\Omega} := [-1, 1]^3$, to individual (curvilinear-brick) elements Ω^e , $e = 1, \dots, E$. On $\hat{\Omega}$, solutions are represented in terms of N th-order tensor-product polynomials,

$$\mathbf{u}(\mathbf{x})|_{\Omega^e} = \sum_{i=0}^N \sum_{j=0}^N \sum_{k=0}^N \mathbf{u}_{ijk}^e h_i(r) h_j(s) h_k(t), \quad (3)$$

where the h_i s are stable nodal interpolants based on the Gauss-Lobatto-Legendre quadrature points $(\xi_i, \xi_j, \xi_k) \in \hat{\Omega}$ and $\mathbf{x} = \mathbf{x}^e(r, s, t)$ maps to Ω^e . This form allows all operator evaluations to be expressed as *fast tensor contractions*, which can be implemented as BLAS3 operations [3] in only $O(N^4)$ work and $O(N^3)$ memory references [17, 18]. This low complexity is in sharp contrast to the $O(N^6)$ work and storage complexity of the traditional p -type FEM. Moreover, hexahedral (hex) element function evaluation is about six times faster per degree-of-freedom (dof) than tensor-based tetrahedral (tet) operator evaluation [19]. By diagonalizing one direction at a time, the SEM structure admits fast (exact or inexact) block solvers for local Poisson problems, which serve as local smoothers for p -multigrid (pMG) [20]. C^0 continuity implies that the SEM is *communication minimal*: data exchanges have unit-depth stencils, independent of N . Local i - j - k indexing avoids much of the indirect addressing associated with fully unstructured approaches, such that high-order SEM implementations can realize significantly higher throughput (millions of dofs per second) than their low-order counterparts [21]. The $O(N)$ computational intensity of the SEM brings direct benefits because its rapid convergence allows one to accurately simulate flows with fewer gridpoints than lower-order discretizations. Again in the regime of high-fidelity simulation of turbulence, the asymptotic error behavior of the SEM, $C = O(h^N)$, manifests its advantage. It is more efficient to increase N than to decrease the grid spacing, $h = O(E^{-\frac{1}{3}})$.

Codes that are comparable in scalability to NekRS include: Nektar [19], which employs the Nek5000 communication kernel, *gslib* and is based primarily on tets; libParanumal[22]; NUMO[23]; Neko[24];

deal.ii [25]; and MFEM [26], with the latter two having CPU kernel performance comparable to Nek5000 [21].

3. Advanced Algorithms

A novel aspect of the current simulations is the use of **high-order overset grids on GPUs**, which has recently been ported to NekRS following work by Lindquist [27]. The overset approach is basically a Schwarz overlapping method applied to the NSE. At each timestep, each *session* (or grid), s , advances the NSE independently on domain Ω_s having boundary $\partial\Omega_s$. Following [28], boundary data on segments of $\partial\Omega_s$ that intersect another domain, $\Omega_{s'}$, is computed as a k th-order extrapolant (in time) of the data from $\Omega_{s'}$. For stability, it is necessary to iterate (i.e., via a predictor-corrector scheme) on the linear Stokes subset of the NS advancement when $k > 0$. Simply using the data from the prior timestep (i.e., $k = 0$) is, however, sufficient for most turbulent flows with no observable impact on turbulence statistics. This approach was developed in earlier work for Nek5000 [29, 30, 28, 31]. It is similar to the overset grid technology that is well established in other codes (e.g., [32, 33]) and that has been ported to GPUs in more recent works (e.g., [34, 35, 36]).

Central to the Nek5000/RS overset implementation is the scalable interpolation library, *findpts()*, written by James Lottes. Designed for millions of processors, this routine allows any MPI rank to post an interpolation query for any $\mathbf{x}^* \in \mathbb{R}^d$ and returns to this rank the value of the requested fields at \mathbf{x}^* . (Void if $\mathbf{x}^* \notin \Omega$.) *findpts()* has three components: (i) a local setup, which identifies the mesh geometry on each rank; (ii) a nonlocal “find-points” call, which returns to the query-rank the MPI rank, element number, and local coordinates $\mathbf{r}^* \in \hat{\Omega}$ corresponding to \mathbf{x}^* ; and (iii) an evaluation call, *findpts_eval(u)*, which returns the value of scalar or vector fields at \mathbf{x}^* . These calls are made *en masse* (multiple queries from multiple processors) and data exchanges are effected in $\log P$ time using fast implementations of the generalized all-to-all *crystal router* routine of [37]. Global and local hash tables accelerate the search for the owning MPI rank and owning element, respectively, that contains \mathbf{x}^* . On candidate elements, Ω^e , a Newton iteration identifies the minimizer, $\mathbf{r}^* = \operatorname{argmin}_{\mathbf{r} \in \hat{\Omega}} \|\mathbf{x}^e(\mathbf{r}) - \mathbf{x}^*\|$, to a small multiple of machine precision such that successful interpolations yield the full accuracy of the high-order expansion (3). For static domains, (i)–(ii) are called only once while *findpts_eval(u)* is invoked for each timestep.

In our overset mesh setting, each session (sub-domain) has a different MPI communicator, save for the interpolation step, in which we use a global

communicator in order to leverage the scalable exchange utilities of `findpts()`. The principal work for `findpts_eval()` is evaluation of (3) for each point on the owning processors. Although the interpolation cost is nominally $O(N^3)$ per point, the operation can be cast as a `dgemm` if there are multiple points per element. In NekRS, the main cost is packing and unpacking the relatively small sets of data associated with the subdomain interface points. Sessions in the so-called NekNek coupling typically comprise multiple MPI ranks, with a different communicator assigned to each session. In effect, each session is an independent fluid-thermal simulations. The sessions can differ in their polynomial orders, which means that each session runs an independent executable (multiple-program, multiple-data parallelism). They can also differ in the physical model for each. For example, one session could run a RANS (Reynolds-Averaged Navier Stokes) model, while the other runs LES.

In the present case, we use one session to simulate a conjugate heat transfer (CHT) problem consisting of coolant flow in the passage-ways, coupled with a thin layer of surrounding elements that form part of the supporting solid walls. Because the solid mesh for this simplified CHT problem is simply a skin around the fluid mesh it is easy to construct. To complete the problem, the CHT domain is coupled via overset to a solid-only domain that includes both steel and copper, which are illustrated by the grey and pink regions in Fig. 1. *The overlapping, interpolation-based, coupling greatly simplifies meshing of complex domains because the mesh topologies do not need to be conforming and the surfaces do not need to match precisely.* The solid session solves an unsteady conduction problem that is computationally less demanding than the fluid-thermal CHT problem. The sessions are synchronized by data exchanges at the end of each timestep and the number of ranks assigned to the solid session can be reduced to minimize wait (sync) time. For more general fluid-fluid couplings, details such as mass flux, volume integrals, and multidomain (> 2) interpolation present additional technical issues that have been addressed in [28, 31] that will be supported in NekRS v24.

4. Performance Measurements

At the start of every simulation, NekRS identifies the fastest kernel for each operation through a combination of `MPI_Wtime` and barriers. In this way, OCCA kernels developed for new platforms do not supercede existing ones unless they are actually faster for the given data/platform configuration. The test results are reported for principal kernels in

Table 1: NekRS statistics output for CHT (session 1) case with 26,433,276 fluid elements and 6,440,484 solid elements, each of order $N = 5$, using $P = 1096$ GCDs on Frontier. The solid-only (session 2) results used $E = 55,056,380$ elements and $P = 1720$ GCDs.

```
runtime statistics (step= 2000 totalElapsed= 1037.87s):
```

name	time	abs%	rel%	calls
solve	3.99061e+02s	100.0		
min	1.80199e-01s			
max	6.63928e+00s			
flops/rank	3.56158e+11			
udfExecuteStep	2.82903e-01s	0.1		2000
makef	5.84134e+01s	14.6		2000
makeq	3.12773e+01s	7.8		2000
udfProperties	1.85385e-02s	0.0		2001
neknk	1.10285e+02s	27.6		2000
sync	9.72651e+00s	2.4	8.8	2000
exchange	9.96520e+01s	25.0	90.4	2000
eval kernel	2.49230e+00s	0.6	2.5	4000
velocitySolve	3.87565e+01s	9.7		2000
rhs	5.77085e+00s	1.4	14.9	2000
pressureSolve	1.09136e+02s	27.3		2000
rhs	1.73350e+01s	4.3	15.9	2000
preconditioner	7.43816e+01s	18.6	68.2	2461
PMG smoother	3.40848e+01s	8.5	45.8	4922
PMG smoother	1.49686e+01s	3.8	20.1	4922
coarse grid	2.10594e+01s	5.3	28.3	2461
initial guess	9.22916e+00s	2.3	8.5	2000
scalarSolve	3.01516e+01s	7.6		2000
rhs	4.96832e-01s	0.1	1.6	2000

Table 2: NekRS statistics output for solid (session 2) using $E = 55,056,380$ elements of order $N = 5$ and $P = 1720$ GCDs, corresponding to session 1 of Table 1.

```
runtime statistics (step= 2000 totalElapsed= 1032.63s):
```

name	time	abs%	rel%	calls
solve	3.98246e+02s	100.0		
min	1.71048e-01s			
max	5.95790e+00s			
flops/rank	3.82066e+10			
udfExecuteStep	1.71539e-01s	0.0		2000
makeq	1.90070e+00s	0.5		2000
udfSEqnSource	9.52365e-02s	0.0	5.0	2000
udfProperties	1.76741e-02s	0.0		2001
neknk	1.85230e+02s	46.5		2000
sync	9.12206e+01s	22.9	49.2	2000
exchange	9.33105e+01s	23.4	50.4	2000
eval kernel	3.43530e+00s	0.9	3.7	4000
scalarSolve	3.76495e+01s	9.5		2000
rhs	4.75687e-01s	0.1	1.3	2000

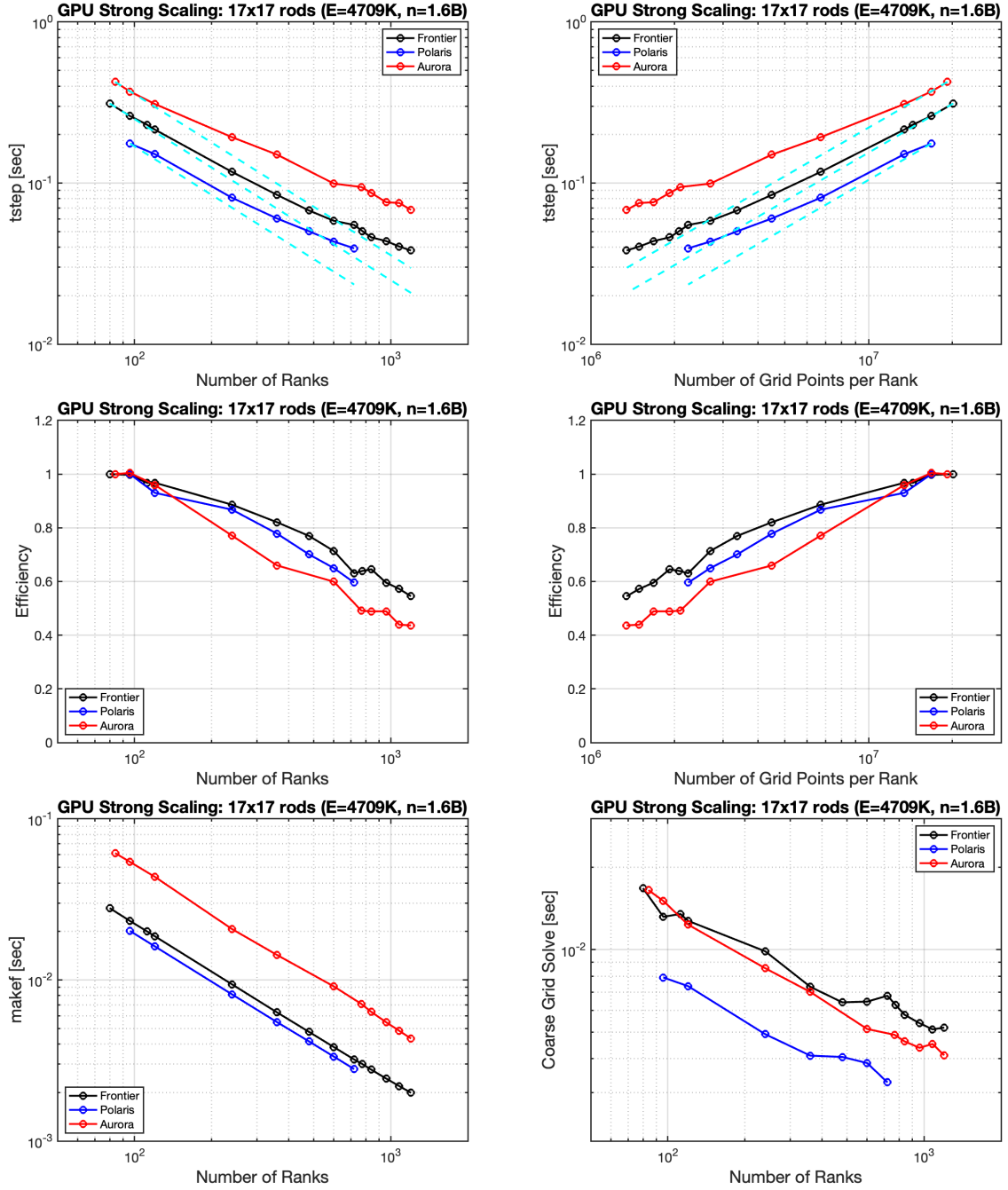


Figure 2: Aurora, Frontier, and Polaris strong-scalings for Navier-Stokes simulation of 17×17 rod bundle using the total number of grid points, $n = 1.6B$. The average (wall) time per step, t_{step} , in seconds is measured over steps 1001–2000. $makef$ is a routine responsible for setting up the right-hand-sides for the momentum equations, involving evaluation of the dealiased advection operator for the velocity.

each logfile and include the operation, degrees-of-freedom per second (GDOFS), precision (FP32/64), bandwidth (GB/s), performance (GFLOPS), and chosen kernel version. Inspection of these tables is extremely useful in identifying under-performing kernels as platforms change.

A similar battery of tests is used to select communication patterns. For example, data might be packed and exchanged on the device using GPU-aware MPI, or it might be packed on the device and exchanged via the host, or packed and exchanged on the host. (Short messages tend to favor this latter option.) The exchanges are tested stand-alone or in conjunction with overlapped computation, depending on the kernel in question. Overlapping communication with computation typically yields a 10–15% reduction in Navier-Stokes solution time. Similarly, using FP32 in the preconditioners reduces memory and network bandwidth pressure and yields another 10–15% savings. (All reported FLOPS are for FP64, with FP32 floating point operations counted as a 1/2 FLOP.)

NekRS is fully instrumented to track basic run-time statistics, which are output every 500 time steps unless the user specifies otherwise. Timing breakdowns follow the physical substeps of advection, pressure, and viscous update, plus tracking of known communication bottlenecks such as the coarse-grid solve for the pressure Poisson problem. For the overset grid case there are two (or more) logfiles and the statistics report the synchronization (load imbalance or wait-time) overhead as well as the exchange costs, which includes data packing and interpolation. Table 1 illustrates the output for an overset grid case and how it can be used in guiding performance optimization. First off, we see that each of the 1096 GCDs (2 GCDs per AMD MI250X on OLCF’s Frontier supercomputer), sustains 356 GFLOPS, which is respectable, particularly given the synchronization and communication overhead for the overset grids. In this case, we see that the nonlinear advection operator (`makef`), which is dealiased using $N_q = 11$ quadrature points in each direction, consumes 14.6% of runtime, the overset grid exchange cost (`neknek`) consumes 27.6%, and the pressure solve consumes 27.3% of the time. Here, there are no particular outliers, save for the 27.6% extra `neknek` overhead, which is the price paid for having extreme geometric flexibility. Note that, as demonstrated in [28], the overhead on CPUs is generally lower (< 10%). Unstructured interpolation is not a GPU/SIMD-friendly operation.

Table 2 shows the corresponding output for the solid-only domain, which has $E = 55M$. The most striking feature of this case is that the flop count is quite low, which indicates that fewer ranks could be effectively assigned to this part of the domain.

5. Performance Results

Fission Results. From the logfile timing data, we plot strong-scaling performance in Fig. 2 for a flow through a single 17×17 rod bundle of a fission reactor for $E = 4709K$ elements of order $N = 7$ ($n=1.6B$ gridpoints). Shown in the top row are measured values of the time-per-step for three platforms: OLCF’s Frontier, which features AMD MI250X GPUs, each having two MPI ranks (one per GCD); ALCF’s NVIDIA A100-based Polaris (one rank per A100); and ALCF’s Aurora, which has Intel PVC GPUs, each running two MPI ranks (one per tile). We plot the performance as a function of P , the number of MPI ranks, in the upper left, and as a function of n/P on the upper right. Because it factors out problem size, the number of points per rank is somewhat more universal than the number of ranks as an independent variable [21]. The plots show that Polaris is about $2\times$ faster than Aurora, per rank and about $1.5\times$ faster than Frontier. We expect that the Aurora numbers will improve as network issues are sorted out. The center row shows the parallel efficiency. We see that, for this case, Frontier realizes $\approx 80\%$ efficiency at $n_{0.8} = n/P = 4M$ points per rank, whereas Polaris has $n_{0.8} = 5M$, and Aurora has $n_{0.8} = 7M$. Larger values of $n_{0.8}$ imply that one has to use fewer processors, and thus run slower, to maintain 80% efficiency. (Small $n_{0.8}$ is better.) In all likelihood, Aurora’s numbers will improve once this early system is debugged.

The last row of Fig. 2 breaks out the costs of some of the leading performance bottlenecks. On the lower left, we plot the time-per-step for the nonlinear advection evaluation, `makef`. We see that Aurora spends roughly twice the amount of time in this kernel than either Frontier or Polaris. This kernel shows perfect linear scaling because it is compute intensive and almost devoid of communication. We speculate that the relatively poor performance of Aurora stems from cache effects on the PVC. Because advection is dealiased with the $3/2$ ’s rule, the working data set per element is 12^3 , rather than 8^3 , which is the size for the majority of the other elemental operations. Experiments in which we reduce the order of dealiasing from 12 to 9 for this case led to a $1.5\times$ reduction in advection time, but this is not as dramatic an improvement as one might expect when cache spilling is alleviated. We note that the majority of the Aurora kernel performance is on par with Frontier.

On the lower right of Fig. 2 we plot the coarse-grid solve time per step, which can be significant for large values of P [3]. In contrast to advection, the coarse-grid solve is communication intensive and uses Hypr on the host CPU to solve the unstructured sparse $p = 1$ problem, which has $\approx E$ unknowns. Here, Polaris is $\approx 2\times$ faster than either

Table 3: CHIMERA Cases: nelv=# of fluid elements; nelt=# of thermal-fluid elements

E	N	Type	dt	avg CFL	avg Pr	range	note
21M	3	overset	1×10^{-5}	0.068	1	1001-2000	
21M	4	overset	1×10^{-5}	0.112	1.046	1001-2000	
21M	5	overset	1×10^{-5}	0.165	1.007	1001-2000	
21M	5	overset	1×10^{-4}	1.483	1.046	1001-2000	
51M	7	fluid only	1×10^{-5}	0.534	1	1001-2000	
211M	7	fluid only	2×10^{-4}	1.087	5.216	1001-2000	
1.69B	3	fluid only	5×10^{-4}	1.257	8.099	1001-2000	pproj=8
1.69B	3	fluid only	5×10^{-4}	1.257	7.269	1001-2000	pproj=L30
1.69B	7	fluid only	1×10^{-4}	1.103	50.195	101-300	MG7531-cheb6
1.69B	9	fluid only	5×10^{-5}	0.872	120.55	21-60	MG951-cheb3

Aurora or Frontier. Remarkably, this result indicates that Aurora’s host-to-host network is reasonably fast and perhaps running better than that of Frontier.

Fusion Results. We have constructed a sequence of CHIMERA meshes with and without the overset solid geometry. A subset of these is listed in Table 3. We remark that the smallest of these cases, with $E = 21M$ elements is almost 50% larger than the record Nek5000 problem size of $E = 15M$, which ran on 1M ranks of ALCF’s BG/Q, Mira, at the start of the ECP project in 2017. The sequence in Table 3 is remarkable simply for the sheer size, which scales up to > 1 trillion grid points for the largest case. These meshes were constructed using a tet-to-hex decomposition and the largest two cases were generated using oct-refinement of the next smallest ones.

The table indicates that the number of pressure iterations per step is reasonable (< 10) up to $E = 1.69B$, $N = 7$ ($n = 580B$), where it climbs to > 50 and ultimately to > 120 iterations per step. Unfortunately, these larger cases are full Frontier runs and thus challenging to debug/optimize. We had some success, however, for the $E = 1.69B$, $N = 3$ ($n = 45B$) case, which could be run on a reasonably small subset of Frontier. At each timestep in Nek5000/RS, we generate an initial guess for the pressure (and velocity) by projecting onto the space of prior solutions [38]. This approximation is stable and exponentially convergent with the number of prior solutions saved, with accuracy ultimately controlled by the iteration tolerance. By increasing the number of prior solutions from 8 to 30, the average pressure iteration was reduced from 8.1 to 7.3 to yield an overall 10% reduction in simulation time. There is some hope that similar gains could be realized for the larger cases in the table, particularly where the pressure iteration counts are large. Also, using aggressive p -multigrid schedules of $p = 7, 5, 3$, and 1 with 6th-order Chebyshev smoothing made inroads for the $E = 1.69B$, $N = 7$ case. Nonetheless, the 1 to 2 orders-of-magnitude increase in pressure iterations

is a significant barrier to overcome for problems at this scale; just discovering whether the issue lies in a bug in the mesh, the solver, or the algorithm will require significant human and computational resources. Finally, we remark that the performance for the fluid only cases ranges from 160 GFLOPS/rank for the $E = 1.6B$ cases on $P = 73728$ ranks of Frontier (12 PFLOPS total) to 700 GFLOPS/rank for the $E = 51M$ case on 4000 ranks (2.8 PFLOPS total). The fall-off in per-rank performance is attributable in part to network noise on Frontier and is alleviated to some extent by bypassing the GPU-direct option in NekRS.

Next, we examine strong scalability for overset grids on GPUs for the CHIMERA geometry. Figure 3 (left) shows the time-per-step for a case with $E = 26, 433, 276$ fluid elements and 6,440,484 solid element in session 1. Session 2 has 55,056,380 solid elements. Also shown is a simple monodomain CHT case that is the same as session 1 of the overset grid case. We see that the monodomain case requires about 25% less time per step than the overset grid case. Figure 3 (right) shows the parallel efficiency for these two cases, which indicates that one can use roughly the same number of processors for the overset case as for the monodomain case at the 80% efficiency mark. Also shown is the efficiency for the comparable ZEFR code ($N = 4$) running on the V100s of Summit [35].

6. Implications

Fusion and Fission system designs. The simulations of reactor cores and fusion system devices described here are ushering in a new era for the thermal fluid analysis of such systems. The possibility of simulating these systems in all their size and complexity at this level of fidelity was unthinkable until recently. The simulations are already being used to benchmark and improve predictions obtained with traditional methods. This innovation is particularly crucial for fusion

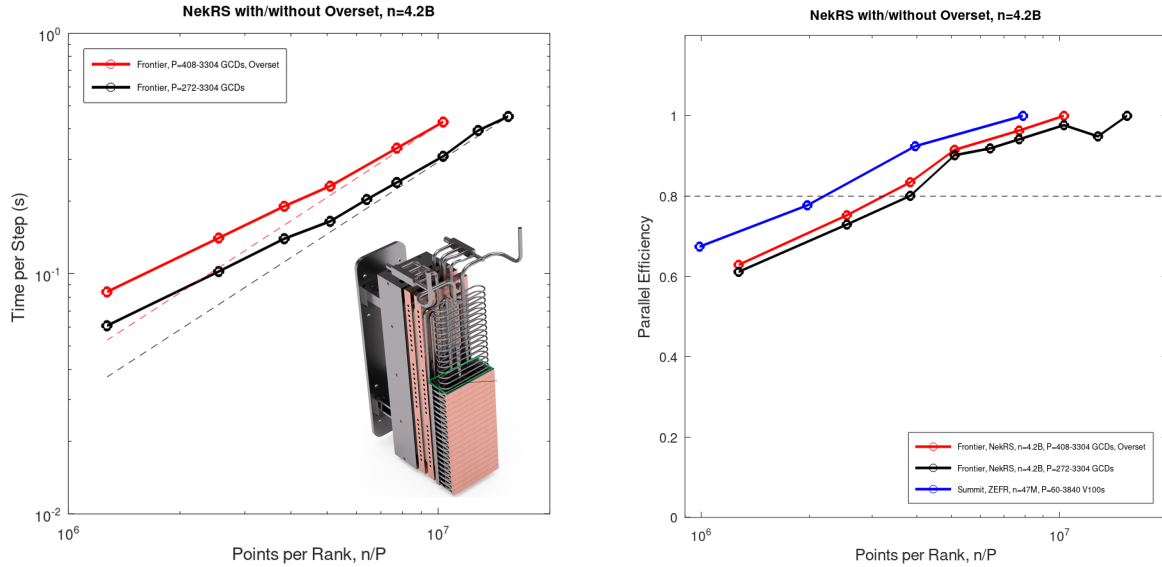


Figure 3: Overset grid results for the CHIMERA geometry (inset). Left: strong-scaling time-per-step for the fluid-thermal (CHT) part of the geometry with and without overset coupling. Right: parallel efficiency for the same cases; also shown is the efficiency for the comparable ZEFR code ($N = 4$) running on the V100s of Summit [35].

blanket systems due to their complexity, lack of existing experimental datasets, and prohibitive heat transfer conditions. Modeling and simulation tools, once validated, can provide a powerful tool to complement experimental data and enable a broader exploration of the design space. We envision that the impact will be increasingly felt as fusion transitions from a physics challenge problem to an engineering challenge problem. This will, in turn, broadly serve the goal of reaching a carbon-free economy within the next few decades.

HPC, Algorithms, and CFD. This study demonstrates the continued importance of numerical algorithms and implementations for HPC, with a several-fold increase in modeling size over a short time frame. Simulations have also increased in complexity (intricate geometry, large problem sizes, overset grids). *Attention to maintaining a performant code base while increasing code and simulation complexity has proven to be essential.* In particular, Automated tuning has proven to be a boon to performance portability since no single approach works for every problem in the parameter space (e.g., spanning polynomial order, local problem size, hardware and software version) as complexity increases. For users, who often have a singular interest, being able to deliver best-in-class performance can be critical to productivity. In Nek5000 and NekRS, we support automated tuning of kernels and communication strategies that adapt to the architecture, problem layout, network, and underlying topology of the particular graph that is invoked at runtime. Performance gains realized through this study will be leveraged

by the 500+ members of the Nek5000/RS user community and will, we hope, establish an approach to portable HPC software running on everything from workstations to exascale platforms and beyond.

Acknowledgments

This material is based upon work supported by the U.S. Department of Energy, Office of Science, under contract DE-AC02-06CH11357 and by the Exascale Computing Project (17-SC-20-SC), a collaborative effort of two U.S. Department of Energy organizations (Office of Science and the National Nuclear Security Administration). The research used resources at the Argonne Leadership Computing Facility at Argonne National Laboratory which is supported by the Office of Science of the U.S. Department of Energy under Contract DE-AC02-06CH11357 and the Oak Ridge Leadership Computing Facility at Oak Ridge National Laboratory, which is supported by the Office of Science of the U.S. Department of Energy under Contract DE-AC05-00OR22725.

References

- [1] E. Merzari, S. Hamilton, T. Evans, M. Min, P. Fischer, S. Kerke-meier, J. Fang, P. Romano, Y.-H. Lan, M. Phillips, et al., Exascale multiphysics nuclear reactor simulations for advanced designs, in: Proceedings of the International Conference for High Performance Computing, Networking, Storage and Analysis, 2023, pp. 1–11.
- [2] M. Min, Y. Lan, P. Fischer, T. Rathnayake, J. Holmen, Nek5000/RS performance on advanced GPU architectures, Frontiers in High Perf. Comput., submitted.

- [3] M. Min, Y. Lan, P. Fischer, E. Merzari, S. Kerkemeier, M. Phillips, T. Rathnayake, A. Novak, D. Gaston, N. Chalmers, T. Warburton, Optimization of full-core reactor simulations on Summit, in: Proc. of SC22: Int. Conf. for High Performance Computing, Networking, Storage and Analysis, IEEE, 2022.
- [4] G. Federici, L. Boccaccini, F. Cismondi, M. Gasparotto, Y. Poitevin, I. Ricapito, An overview of the eu breeding blanket design strategy as an integral part of the demo design effort, Fusion Engineering and Design 141 (2019) 30–42.
- [5] S. Konishi, M. Enoeda, M. Nakamichi, T. Hoshino, A. Ying, S. Sharafat, S. Smolentsev, Functional materials for breeding blankets—status and developments, Nuclear Fusion 57 (9) (2017) 092014.
- [6] T. Barrett, M. Bamford, B. Chuilon, T. Deighan, P. Efthymiou, L. Fletcher, M. Gorley, T. Grant, T. Hall, D. Horsley, et al., The chimera facility development programme, Fusion Engineering and Design 194 (2023) 113689.
- [7] M. Min, J.-S. Camier, P. Fischer, A. Karakus, S. Kerkemeier, T. Kolev, Y.-H. Lan, D. Medina, E. Merzari, A. Obabko, et al., Engage second wave ecp/ceed applications, Tech. rep., Lawrence Livermore National Lab.(LLNL), Livermore, CA (United States) (2018).
- [8] K. Mittal, S. Dutta, P. Fischer, Nonconforming schwarz-spectral element methods for incompressible flow, Computers & Fluids 191 (2019) 104237.
- [9] J. Fang, D. R. Shaver, A. Tomboulides, M. Min, P. Fischer, Y.-H. Lan, R. Rahaman, P. Romano, S. Benhamadouche, Y. A. Hassan, et al., Feasibility of full-core pin resolved cfd simulations of small modular reactor with momentum sources, Nuclear Engineering and Design 378 (2021) 111143.
- [10] A. Patera, A spectral element method for fluid dynamics : laminar flow in a channel expansion, J. Comput. Phys. 54 (1984) 468–488.
- [11] P. Fischer, J. Lottes, S. Kerkemeier, Nek5000: Open source spectral element CFD solver. <http://nek5000.mcs.anl.gov> and <https://github.com/nek5000/nek5000>.
- [12] H. Tufo, P. Fischer, Terascale spectral element algorithms and implementations, in: Proc. of the ACM/IEEE SC99 Conf. on High Performance Networking and Computing, Gordon Bell Prize, IEEE Computer Soc., CDROM, 1999.
- [13] K. Świrydowicz, N. Chalmers, A. Karakus, T. Warburton, Acceleration of tensor-product operations for high-order finite element methods, Int. J. of High Performance Comput. App. 33 (4) (2019) 735–757.
- [14] A. Karakus, N. Chalmers, K. Świrydowicz, T. Warburton, A gpu accelerated discontinuous galerkin incompressible flow solver, J. Comp. Phys. 390 (2019) 380–404.
- [15] D. S. Medina, A. St-Cyr, T. Warburton, OCCA: A unified approach to multi-threading languages, preprint arXiv:1403.0968.
- [16] H. Kreiss, J. Olinger, Comparison of accurate methods for the integration of hyperbolic problems, Tellus 24 (1972) 199–215.
- [17] M. Deville, P. Fischer, E. Mund, High-order methods for incompressible fluid flow, Cambridge University Press, Cambridge, 2002.
- [18] S. Orszag, Spectral methods for problems in complex geometry, J. Comput. Phys. 37 (1980) 70–92.
- [19] D. Moxey, R. Amici, M. Kirby, Efficient matrix-free high-order finite element evaluation for simplicial elements, SIAM J. Sci. Comput. 42 (3) (2020) C97–C123.
- [20] J. W. Lottes, P. F. Fischer, Hybrid multigrid/Schwarz algorithms for the spectral element method, J. Sci. Comput. 24 (2005) 45–78.
- [21] P. Fischer, M. Min, T. Rathnayake, S. Dutta, T. Kolev, V. Dobrev, J.-S. Camier, M. Kronbichler, T. Warburton, K. Świrydowicz, J. Brown, Scalability of high-performance PDE solvers, Int. J. of High Perf. Comp. Appl. 34 (5) (2020) 562–586. [arXiv:https://doi.org/10.1177/1094342020915762](https://doi.org/10.1177/1094342020915762).
- URL <https://doi.org/10.1177/1094342020915762>
- [22] N. Chalmers, A. Karakus, A. P. Austin, K. Świrydowicz, T. Warburton, libParanumal (2020).
- [23] F. Giraldo, The nonhydrostatic unified model of the ocean (numo). <https://frankgiraldo.wixsite.com/mysite/numo>.
- [24] N. Jansson, M. Karp, A. Podobas, S. Markidis, P. Schlatter, Neko: A modern, portable, and scalable framework for high-fidelity computational fluid dynamics, CoRR abs/2107.01243. [arXiv:2107.01243](https://arxiv.org/abs/2107.01243). URL <https://arxiv.org/abs/2107.01243>
- [25] D. Arndt, W. Bangerth, D. Davydov, T. Heister, L. Heltai, M. Kronbichler, M. Maier, J. Pelteret, B. Turcksin, D. Wells, The deal.II library, version 8.5, J. Num. Math. 25 (3) (2017) 137–145. URL www.dealii.org
- [26] R. Anderson, J. Andrej, A. Barker, J. Bramwell, J.-S. Camier, J. C. V. Dobrev, Y. Dudouit, A. Fisher, T. Kolev, W. Pazner, M. Stowell, V. Tomov, I. Akkerman, J. Dahm, D. Medina, S. Zampini, MFEM: A modular finite element library, Computers & Mathematics with Applications doi:10.1016/j.camwa.2020.06.009.
- [27] N. Lindquist, P. Fischer, M. Min, Scalable interpolation on gpus for thermal fluids applications, Technical Report ANL-21/55, Argonne National Laboratory (ANL), Argonne, IL, United States (October 2021).
- [28] K. Mittal, S. Dutta, P. Fischer, Nonconforming Schwarz-spectral element methods for incompressible flow, Computers and Fluids 191.
- [29] Y. Peet, P. Fischer, Stability analysis of interface temporal discretization in grid overlapping methods, SIAM J. Numer. Anal. 50 (2012) 3375–3401.
- [30] B. Merrill, Y. Peet, P. Fischer, J. Lottes, A spectrally accurate method for overlapping grid solution of incompressible Navier-Stokes equations, J. Comput. Phys. 307 (2016) 60–93.
- [31] K. Mittal, S. Dutta, P. Fischer, Stability analysis of a singlerate and multirate predictor-corrector scheme for overlapping grids, arXiv preprint arXiv:2010.00118.
- [32] J. L. Steger, F. C. Dougherty, J. A. Benek, A chimera grid scheme.[multiple overset body-conforming mesh system for finite difference adaptation to complex aircraft configurations].
- [33] F. Bassetti, D. Brown, K. Davis, W. Henshaw, D. Quinlan, OVERTURE: An object-oriented framework for high-performance scientific computing, in: Proceedings of Supercomputing’98 (CD-ROM), ACM SIGARCH and IEEE, 1998.
- [34] D. Chandar, J. Sitarman, D. J. Mavriplis, A hybrid multi-GPU/CPU computational framework for rotorcraft flows on unstructured overset grids, in: 21st AIAA Comp. Fluid Dyn. Conf., AIAA, San Diego, 2013, pp. AIAA Paper 2013–2855.
- [35] J. Romero, J. Crabill, J. Watkins, F. Witherden, A. Jameson, ZEFR: A GPU-accelerated high-order solver for compressible viscous flows using the flux reconstruction method, Comp. Phys. Comm. 250 (2020) 107169.
- [36] C. Jackson, D. Appelhans, J. Derlaga, P. Buning, GPU implementation of the OVERFLOW CFD code, in: AIAA SciTech Forum and Expo, AIAA, Langley Research Center, Orlando, FL, 2024, document ID: 20230016176.
- [37] G. C. Fox, M. A. Johnson, G. A. Lyzenga, S. W. Otto, J. K. Salmon, D. W. Walker, Solving Problems on Concurrent Processors, Prentice-Hall, Englewood Cliffs, NJ, 1988.
- [38] P. Fischer, Projection techniques for iterative solution of $A\bar{x} = \bar{b}$ with successive right-hand sides, Comput. Methods Appl. Mech. Engrg. 163 (1998) 193–204.